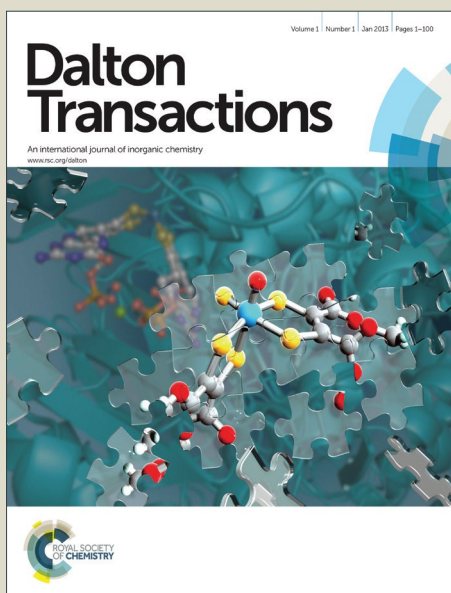


# Dalton Transactions

Accepted Manuscript



This is an *Accepted Manuscript*, which has been through the Royal Society of Chemistry peer review process and has been accepted for publication.

*Accepted Manuscripts* are published online shortly after acceptance, before technical editing, formatting and proof reading. Using this free service, authors can make their results available to the community, in citable form, before we publish the edited article. We will replace this *Accepted Manuscript* with the edited and formatted *Advance Article* as soon as it is available.

You can find more information about *Accepted Manuscripts* in the [Information for Authors](#).

Please note that technical editing may introduce minor changes to the text and/or graphics, which may alter content. The journal's standard [Terms & Conditions](#) and the [Ethical guidelines](#) still apply. In no event shall the Royal Society of Chemistry be held responsible for any errors or omissions in this *Accepted Manuscript* or any consequences arising from the use of any information it contains.



Journal Name

ARTICLE

## Solvent triggered structural diversity of triple-stranded helicates: single molecular magnets†

Hongfeng Li, Peng Chen,\* Wenbin Sun, Lei Zhang and Pengfei Yan\*

Received 00th January 20xx,  
Accepted 00th January 20xx

DOI: 10.1039/x0xx00000x

www.rsc.org/

Multiple-stranded helicates are speculated in respect to their simplicity in geometry and significance in the biology and materials. Bis- $\beta$ -diketones have shown their advantage in the structure and geometry in the construction of multiple-stranded helicates, but further studies on their properties are limited due to their poor crystallization. In this study, the solvents are found to have played decisive role in the crystallization of triple-stranded helicate.  $[\text{Dy}_2(\text{BTB})_3(\text{H}_2\text{O})_4]$  is used as a precursor to solvent-dependently crystallize three complexes  $[\text{Dy}_2(\text{BTB})_3(\text{CH}_3\text{OH})_4] \cdot 3\text{CH}_3\text{OH}$  (**1**),  $[\text{Dy}_2(\text{BTB})_3(\text{DME})_2]$  (**2**) and  $[\text{Dy}_2(\text{BTB})_3(\text{DOA})(\text{H}_2\text{O})_2] \cdot 4.5\text{DOA}$  (**3**) (BTB = 3,3'-bis(4,4,4-trifluoro-1,3-dioxobutyl)biphenyl), where the key structural motif of the triple-stranded helicate  $[\text{Dy}_2(\text{BTB})_3]$  is retained. Four methanol molecules are found to ligate to  $\text{Dy}^{3+}$  ions in **1**, while each  $\text{Dy}^{3+}$  ion is chelated by one DME molecule in **2**. Interestingly, it is observed that 1,4-dioxane as a bridge ligates to two adjacent  $\text{Dy}^{3+}$  ions, giving rise to the formation of a 1D chain structure. Magnetic measurement shows that **1** and **2** display slow magnetic relaxation under zero dc field, while single molecular magnet behavior is obtained for **3** under an applied dc field of 2000 Oe.

### Introduction

Helical structures are widely found and investigated in the fields of botany, biology and materials, ever since the double helical structure of DNA was elucidated.<sup>1</sup> Thereafter, chemists have been devoted to the synthetic work in the pursuit of the potential helical materials, and diversified ligands in different lengths, sequences and coordination modes have been designed and employed for the construction of multi-stranded helicates on both transition metals and lanthanides.<sup>2,3</sup> On account of their preferential bidentate chelating modes to lanthanides, the bis- $\beta$ -diketones have recently been utilized to construct the multiple-stranded helicates, where intriguing fluorescent and magnetic properties could be expected.<sup>2e,4</sup>

Nowadays, it has been proven effective for the  $\beta$ -diketonate-Dy strategy in the construction of the single molecular magnets (SMM) with larger energy barrier,<sup>4b,5</sup> while the  $\text{Dy}^{3+}$  ion is approximately situated in a  $D_{4d}$  symmetry.<sup>6</sup> It is well-known that the ligand field and coordination geometry impose critical influences on the local magnetic anisotropy of the  $\text{Dy}^{3+}$  ions. It remains a challenge to control the coordination geometry around the lanthanide centers

because of their adaption to the various coordination environments. One applicable approach to control the local coordination geometry is to ligate to the central  $\text{Dy}^{3+}$  ion with different auxiliary ligands,<sup>4b</sup> which enables the in-depth understanding on the relationship of the structures and magnetic properties, especially for those with subtle differences in geometry.

Control over the synthetic route and crystallization conditions should be of great importance for the rational formation of polymorphs and supramolecular isomers, providing deeper insights into the design and preparation of the new materials.<sup>7-9</sup> Generally, the resulting structures are determined by several factors, and the changes in the crystallization conditions such as the solvent, pH, the type of the counterion, temperature etc., may be responsible for the development of distinct polymorphic species.<sup>10-13</sup> In particular, the solvents as an important factor has been proven to have significant impact on the crystallization process and on the final structure of the products,<sup>14</sup> which contributes to the structural diversities and structurally-related properties as well.

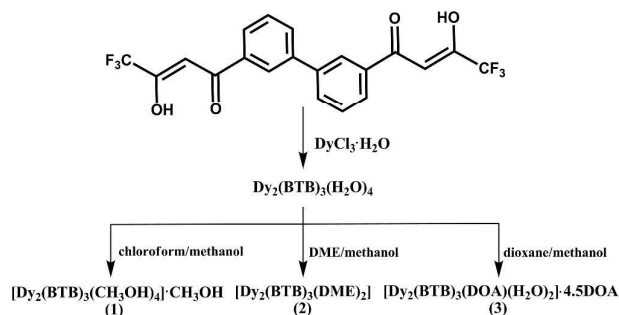
Recently, we have been focusing on the syntheses of multiple-stranded bis- $\beta$ -diketonate-Ln helicates through the design and functionalization on the ligands.<sup>4,15</sup> It is supposed that  $[\text{Dy}_2(\text{BTB})_3(\text{H}_2\text{O})_4]$  could be superior as a basic structural motif to be modified that the water molecules are potentially allowed for the replacement by other proper solvents.<sup>4c</sup> As can be speculated, structural diversity and subtle geometric difference are promised. It highlights the importance of the crystal engineering on the bis- $\beta$ -diketonate-Dy complexes that the absence of crystallographic structure previously stemmed the further investigation and prediction on the structure and property. In this paper, we present the syntheses, crystallization and magnetic properties of three complexes  $[\text{Dy}_2(\text{BTB})_3(\text{CH}_3\text{OH})_4] \cdot 3\text{CH}_3\text{OH}$  (**1**),  $[\text{Dy}_2(\text{BTB})_3(\text{DME})_2]$  (**2**)

Key Laboratory of Functional Inorganic Material Chemistry (MOE), School of Chemistry and Materials Science, Heilongjiang University, Harbin 150080, P.R. China. E-mail: jehugu@gmail.com (Chen P.); yanpf@vip.sina.com (Yan P.).

† Electronic Supplementary Information (ESI) available: Selected bond lengths of **1–3** are listed in Table S1. TG curves are given as Figure S1–S4. The magnetic data are presented as Figure S8–S19. CCDC: 1424064–6. For ESI and crystallographic data in CIF or other electronic format See DOI:10.1039/x0xx00000x

and  $[\text{Dy}_2(\text{BTB})_3(\text{DOA})(\text{H}_2\text{O})_2] \cdot 4.5\text{DOA}$  (**3**) by using  $[\text{Dy}_2(\text{BTB})_3(\text{H}_2\text{O})_4]$  as the precursor (Scheme 1). In **1**, four methanol molecules are

carrier atoms. The experimental details for the structural determination are presented in Table 1.



**Scheme 1** The structure of the ligand  $\text{H}_2\text{BTB}$  and the synthetic routes for **1–3**.

coordinated to  $\text{Dy}^{3+}$  ions, while the  $\text{Dy}^{3+}$  ions are chelated by DME in **2**. Interestingly, DOA molecules bridge two triple-stranded motifs to construct up a 1D chain. Magnetic measurement shows that **1** and **2** display slow magnetic relaxation under zero dc field, while single molecular magnet behavior is obtained for **3** under an applied dc field of 2000 Oe.

## Experimental Section

### Materials and instrumentation

The ligand  $\text{H}_2\text{BTB}$  was prepared according to the reported method ( $\text{H}_2\text{BTB} = 3,3'$ -bis(4,4,4-trifluoro-1,3-dioxobutyl)biphenyl).<sup>4c</sup> Elemental analyses were performed on an Elementar Vario EL cube analyzer. FT-IR spectra were obtained on a Perkin-Elmer Spectrum One spectrophotometer by using KBr disks in the range of 4000–370  $\text{cm}^{-1}$ . The magnetic susceptibility measurements were obtained using a Quantum Design SQUID magnetometer MPMS-3 operating between 2 and 300 K for dc-applied fields ranging from –7 to 7 T, ac susceptibility measurements were carried out under an oscillating ac field of 2 Oe and ac frequencies ranging from 1 to 1000 Hz. A diamagnetic correction was applied for the sample holder. Thermogravimetric analyses were obtained on an SDT Q600 thermogravimetric analyzer at a heating rate of 20  $^\circ\text{C}/\text{min}$  under air atmosphere in the temperature range of 25–780  $^\circ\text{C}$ . All measurements were carried out by using fresh crystals. Single crystals of **1–3** were selected for X-ray diffraction analysis on a Xcalibur, Eos diffractometer using graphite-monochromated  $\text{Mo-K}\alpha$  radiation ( $\lambda = 0.71073 \text{ \AA}$ ). The crystals were kept under  $\text{N}_2$  atmosphere at 150 K during data collection. The structures were solved by the direct methods and refined on  $F^2$  by full-matrix least-square using the ShelXL2014 program.<sup>16</sup> The  $\text{Dy}^{3+}$  ions were firstly located, and then non-hydrogen atoms (C, O and F) were placed from the subsequent Fourier-difference maps and refined anisotropically. In the case of **1**, F10–F12, F16–F18, C64–C67 and O16 atoms have been modelled as disordered with the equivalent occupancy. In the case of **2**, F1–F3 and C1 atoms were found to be disordered with the equivalent occupancy. In the case of **3**, the similar treatment has been applied for atoms (C69–C73, C74–C76, C78–C82, F4–F6, F10–F12 and F16–F18) with the equivalent occupancy. The H atoms were introduced in the calculated positions and refined with fixed geometry with respect to their

**Table 1** Crystal data and structural refinement parameters for 1–3.

Identification	1	2	3
Empirical formula	C <sub>67</sub> H <sub>58</sub> Dy <sub>2</sub> F <sub>18</sub> O <sub>19</sub>	C <sub>68</sub> H <sub>50</sub> Dy <sub>2</sub> F <sub>18</sub> O <sub>16</sub>	C <sub>82</sub> H <sub>78</sub> Dy <sub>2</sub> F <sub>18</sub> O <sub>25</sub>
Formula weight	1834.13	1790.08	2130.44
Cryst. syst.	triclinic	triclinic	triclinic
Space group	<i>P</i> -1	<i>P</i> -1	<i>P</i> -1
<i>a</i> (Å)	11.7570(4)	10.9663(4)	14.7143(3)
<i>b</i> (Å)	18.3880(7)	17.7641(4)	15.2959(3)
<i>c</i> (Å)	18.4659(7)	18.9915(6)	20.6256(5)
$\alpha$ (°)	82.140(3)	94.042(2)	82.262(2)
$\beta$ (°)	72.251(2)	101.496(3)	72.683(2)
$\gamma$ (°)	72.692(2)	103.186(3)	80.0374(19)
Volume (Å <sup>3</sup> )	3625.3(2)	3503.70(19)	4347.85(18)
<i>Z</i>	2	2	2
<i>R</i> <sub>int</sub>	0.0369	0.0282	0.0298
GOF of <i>F</i> <sup>2</sup>	1.159	1.123	1.072
Final <i>R</i>	<i>R</i> <sub>1</sub> = 0.1126	<i>R</i> <sub>1</sub> = 0.0569	<i>R</i> <sub>1</sub> = 0.0391
[>2 $\sigma$ ( <i>I</i> )] indices	w <i>R</i> <sub>2</sub> = 0.2270	w <i>R</i> <sub>2</sub> = 0.1263	w <i>R</i> <sub>2</sub> = 0.0856
<i>R</i> indices (all data)	<i>R</i> <sub>1</sub> = 0.1319 w <i>R</i> <sub>2</sub> = 0.2385	<i>R</i> <sub>1</sub> = 0.0770 w <i>R</i> <sub>2</sub> = 0.1349	<i>R</i> <sub>1</sub> = 0.0593 w <i>R</i> <sub>2</sub> = 0.0966

### Syntheses

0.060 g DyCl<sub>3</sub>·6H<sub>2</sub>O, 0.100 g H<sub>2</sub>BTB and 0.018 g NaOH were refluxed in a mixed solution of MeOH (5mL) and water (5 mL) for 3h. The solution was kept stirred for extra 24 hours, when it was cooled to room temperature. The addition of deionized water led to the white precipitate, which was filtered, collected and dried under vacuum. Thermogravimetric analysis on the precipitate indicated that the empirical formula was Dy<sub>2</sub>(BTB)<sub>3</sub>(H<sub>2</sub>O)<sub>4</sub> (Fig. S1). In the first stage, a weight loss of 4.48 wt% (calcd. 4.27 wt%) was detected corresponding to the removal of four water molecules. Consequently, the second stage occurring at 300 degree was ascribed to the removal of one ligand until 420 degree (found 25.36 wt%, calcd. 25.46 wt%). The last stage was owing the removal of the rest two ligands, and a total weight loss of 77.97 wt% was found in good agreement with the theoretical value of 77.89 wt% for the precipitate. Single crystals of 1–3 suitable for X-ray analysis were obtained by slow diffusion of *n*-hexane into the chloroform/methanol, DME/methanol and DOA/methanol solution of the precipitate in 7 days, respectively (DME = dimethyl ether and DOA = 1,4-dioxane). The thermogravimetric analyses on the fresh crystals of 1–3 were conducted as well (Fig. S2–S4).

#### [Dy<sub>2</sub>(BTB)<sub>3</sub>(CH<sub>3</sub>OH)<sub>4</sub>·3CH<sub>3</sub>OH (1)]

Anal. Calcd. for C<sub>67</sub>H<sub>58</sub>Dy<sub>2</sub>F<sub>18</sub>O<sub>19</sub> (1834.13): C, 43.87; H, 3.19 wt%. Found: C, 43.69; H, 3.11 wt%. IR (KBr, cm<sup>-1</sup>): 3435, 1622, 1534, 1517, 1475, 1298.

#### [Dy<sub>2</sub>(BTB)<sub>3</sub>(DME)<sub>2</sub>] (2)

Anal. Calcd. for C<sub>68</sub>H<sub>50</sub>Dy<sub>2</sub>F<sub>18</sub>O<sub>16</sub> (1790.08): C, 45.63; H, 2.82 wt%. Found: C, 45.65; H, 2.78 wt%. IR (KBr, cm<sup>-1</sup>): 3058, 2964, 1617, 1533, 1475, 1464, 1292.

#### [Dy<sub>2</sub>(BTB)<sub>3</sub>(DOA)(H<sub>2</sub>O)<sub>2</sub>·4.5DOA (3)]

Anal. Calcd. for C<sub>82</sub>H<sub>78</sub>Dy<sub>2</sub>F<sub>18</sub>O<sub>25</sub> (2130.44): C, 46.23; H, 3.69 wt%. Found: C, 46.09; H, 3.61 wt%. IR (KBr, cm<sup>-1</sup>): 3441, 2960, 2851, 1450, 1368, 1295, 1267, 1118.

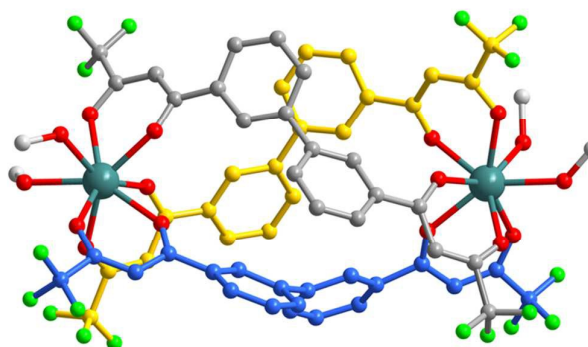


**Fig. 1** The molecular structure of **1** (The C atoms in each ligand are marked in a different colour. H atoms, second sites of disordered parts and guest species have been omitted for clarity).

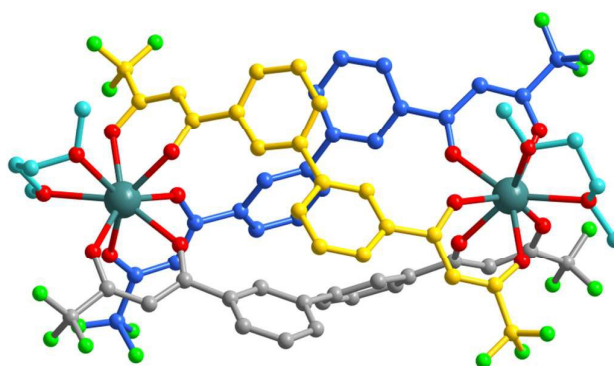


**Fig. 2** The molecular structure of **2** (The C atoms in each ligand are marked in a different colour. H atoms, second sites of disordered parts and guest species have been omitted for clarity).

## Results and discussion

The structural analysis shows that **1** crystallizing in the triclinic space group of *P*-1 is a triple-stranded dinuclear helicate (Fig. 1). In the asymmetric unit of **1**, there are two Dy centers, three BTB ligands and seven methanol molecules. It gives rise to the formation of the triple-stranded helicate that three deprotonated BTB are wrapping about two Dy<sup>3+</sup> ions. Each crystallographically distinct Dy<sup>3+</sup> ion is eight-coordinated to six O atoms of three BTB and two O atoms of two methanol molecules in the square antiprism geometry (Fig. S5).<sup>17</sup> The Dy–O distances are in the range of 2.351(9)–2.489(11) Å, which are in accordance with the reported values. The geometry of each Dy<sup>3+</sup> centers is slightly different and detailed bond lengths are listed in Table S1. There are two Dy<sub>2</sub>(BTB)<sub>3</sub>(CH<sub>3</sub>OH)<sub>4</sub> units in the unit cell that each helicate has homochiral Dy<sup>3+</sup> centers in either a left-handed  $\Lambda$ - $\Lambda$  or right-handed  $\Delta$ - $\Delta$  helix, while the similar results have also been observed for **2** and **3**. The dihedral angles between the two phenyl groups in each BTB are in the range of 48.3–55.2°. The Dy...Dy distance in the same helicate of **1** is 11.9 Å, which is comparable to the reported value.<sup>4c</sup>

Extensive H-bonds are observed among the terminal methanol and dissociative methanol molecules.

**2** crystallizes in the triclinic space group of  $P\bar{1}$  as well, and the structural analysis indicates that **2** possesses similar helical structure (Fig. 2). In the asymmetric unit of **2**, there are two  $\text{Dy}^{3+}$  ions, three BTB ligands and two DME molecules. Each crystallographically distinct  $\text{Dy}^{3+}$  ion is eight-coordinated to six oxygen atoms of three BTB, besides of two O atom of DME (Fig. S6). Each crystallographically distinct  $\text{Dy}^{3+}$  ion is chelated by two DME molecules, in contrast to the methanol in **1**. The Dy–O distances are in the range of 2.289(6)–2.576(6) Å, while the Dy–O (ether O atoms) distances are significantly longer. The dihedral angles between the two phenyl groups in each MBDA are in the range of 45.3–61.2°. The Dy...Dy distance in the same helicate of **2** is 11.9 Å as well. It is

supposed that the weak C–H...F interactions dominate the intermolecular bondings as we have previously discussed.<sup>4a-4c</sup>

The structural analysis on **3** reveals the crystallization of the chain structure in the triclinic space group of  $P\bar{1}$  (Fig. 3). Similar structural motif of  $[\text{Dy}_2(\text{BTB})_3]$  is detected in **3** as well as in **1** and **2**. The two crystallographically independent  $\text{Dy}^{3+}$  ions are ligated to six O atoms of three BTB, one O atom of water and one O atom of DOA (Fig. S7). The Dy–O distances are in the range of 2.292(3)–2.495(3) Å, while the Dy–O (O atoms of water and DOA molecules) distances are significantly longer. The dihedral angles between the two phenyl groups in each BTB are in the range of 40.3–65.3°. Interestingly, DOA molecules serving as a bridge are coordinated to two  $\text{Dy}^{3+}$  ions of two

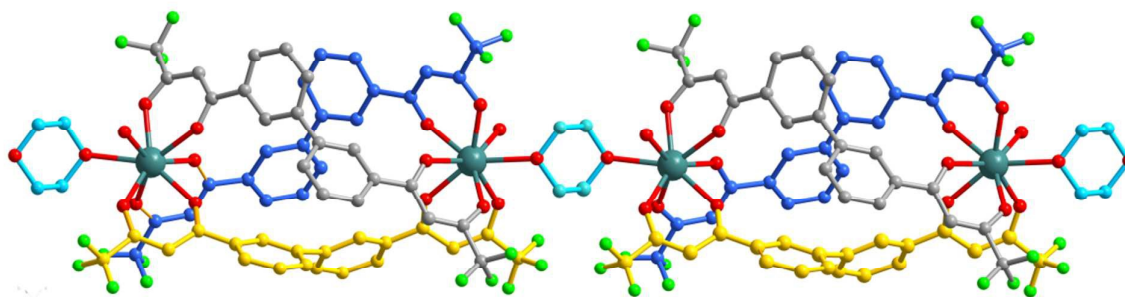


**Fig. 3** The 1D chain structure of **3** is constituted up from the adjacent helicates through the bridging DOA molecules (The C atoms in each ligand are marked in a different colour. H atoms, second sites of disordered parts and guest species have been omitted for clarity).

crystallographically equivalent  $[\text{Dy}_2(\text{BTB})_3(\text{H}_2\text{O})_2]$  moieties, giving rise to the formation of a 1D chain structure (Fig. 3). The water molecules attached to  $\text{Dy}^{3+}$  ions forms H-bondings with the adjacent DOA molecules, which fill up the intermolecular space in **3**. The Dy...Dy distance is 11.9 Å in **3**. It is noted that it is far enough to exclude the intramolecular magnetic coupling for all three cases.

As we have discussed, the insufficiency in the flexibility of BTB ligand would result in the formation of triple-stranded helicate in accordance with the thermogravimetric analysis on the precursor.<sup>4b,4c</sup> The two  $\text{Dy}^{3+}$  ions are supposed to be coordinated to two O atoms of waters, besides of six O atom of three BTB ligands. It is noted that our attempt to crystallize the precursor failed. Meanwhile, less attention has been drawn on the crystallization and the formation of diversified structures of multiple-stranded Ln-bis- $\beta$ -diketonate helicates.<sup>4</sup> The studies on the crystal engineering would be of significance for the host-guest chemistry and their functional behavior arisen from.<sup>18-19</sup> The coordination of waters to  $\text{Dy}^{3+}$  indicates the possibility to be replaced with other solvent molecules, which would simultaneously allow for the formation of diversified structures maintaining its helical structural motif. Thus, various auxiliary ligands and solvents, which could potentially ligate to  $\text{Dy}^{3+}$  centers, have been utilized in the pursuit of stable crystals. And three complexes **1-3** have been obtained with  $\text{CH}_3\text{OH}$ , DME and DOA, respectively. In the structure of **1-3**, conformations of the ligands are dependent on the steric hindrance of the solvents introduced, while the bond angles and the dihedral angles between

the two phenyl groups in each BTB are significantly changed. In contrast to the rigid ligand phenanthroline with fixed geometry, DME in a certain shape would timely adjust their configuration to strengthen the structural stability, while our attempt with phenanthroline failed. Additionally, weak C–H...F and F...F interactions are believed to contribute to the structural stability in all three cases.<sup>4b,20</sup>

#### Magnetic properties of 1-3

The direct-current (dc) magnetic measurements are performed in an applied magnetic field of 1000 Oe (Fig. 4) for **1-3** in the temperature range of 1.8–300 K. At the room temperature, the values of  $\chi T$  are 28.06, 28.15 and 28.22  $\text{cm}^3 \text{K mol}^{-1}$  for **1-3**, respectively, which are close to the expected value for two independent  $\text{Dy}^{3+}$  ions (28.34  $\text{cm}^3 \text{K mol}^{-1}$ ):  $\text{Dy}^{3+}$  ( $S = 5/2$ ,  $L = 5$ ,  $^6\text{H}_{15/2}$ ,  $g = 4/3$ ,  $C = 14.17 \text{ cm}^3 \text{K mol}^{-1}$ ). For the case of **1**, the  $\chi T$  product remained constant down to 75 K on lowering the temperature before dropping rapidly down to 21.72  $\text{cm}^3 \text{K mol}^{-1}$  at 1.8 K. The decrease of  $\chi T$  at low temperature obviously suggests the presence of intramolecular antiferromagnetic interactions within  $\text{Dy}^{3+}$  ions. Similar results can be observed for **2** and **3**. The  $\chi T$  products gradually decrease on lowering the temperature and drop to minimum values of 21.55 and 19.32  $\text{cm}^3 \text{K mol}^{-1}$  at 2 K. The gradual decrease before 75 K is due to the thermal depopulation of the Stark sublevels, whereas the latter rapid drop may be ascribed to the weak antiferromagnetic interactions between the  $\text{Dy}^{3+}$  centers, even if magnetic anisotropy might also partially affect low temperature susceptibility.

Magnetization ( $M$ ) data for **1–3** are collected in the 0–7 T field range below 5 K (Fig. S8–S10). For **1–3**, the magnetization *versus*  $H/T$  data at different temperatures show nonsuperposition plots, and a gradual increase of the magnetization at high fields, without a saturation even at 7 T, revealing the presence of a significant

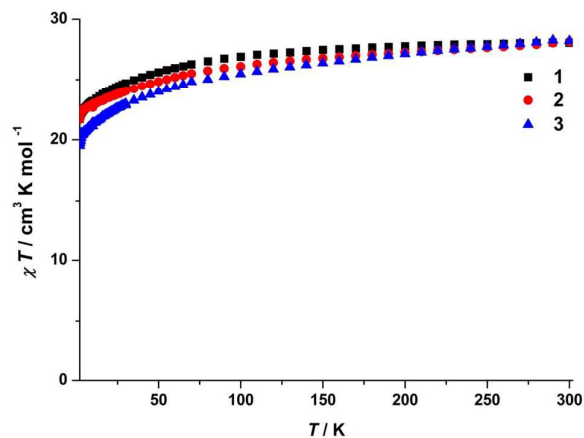


**Fig. 4** Plot of  $\chi T$  vs  $T$  for **1–3** in an applied dc field of 1000 Oe in the temperature range of 1.8–300 K.

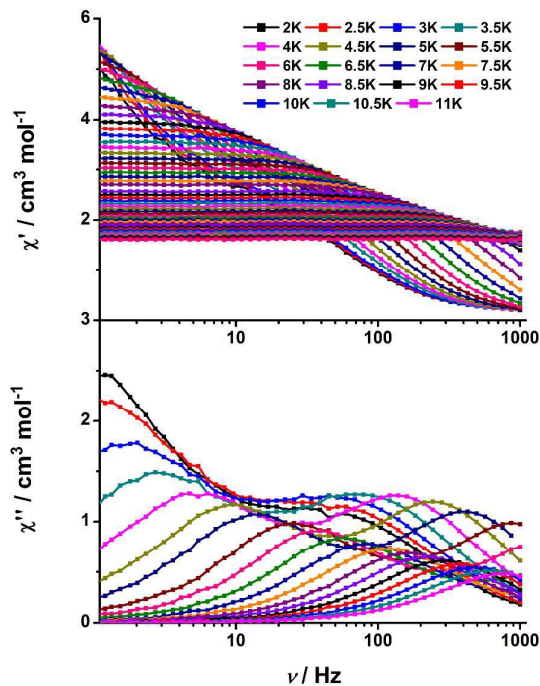


**Fig. 5** Frequency dependence of the in-phase ( $\chi'$ , top) and the out-of-phase ( $\chi''$ , bottom) ac susceptibilities for **2** under 2000 Oe dc field in the temperature range of 2–11 K.

magnetic anisotropy and/or low-lying excited states. The dynamics of the magnetization for **1–3** are investigated using alternating current susceptibility measurements. A temperature dependent increase of the in-phase signal with the appearance of an out-of-

phase signal is observed for **1** and **2**, while no distinct signals are found for **3** (Fig. S11–S13). The increasing of  $\chi'$  and  $\chi''$  below 4 K is indicative of the quantum tunnelling of the magnetization (QTM) at a zero dc field, which is typical properties for the lanthanide-based SMMs. (Fig. S14–S16). To suppress the QTM effect, ac susceptibility measurements are performed under a static dc field of 2000 Oe for

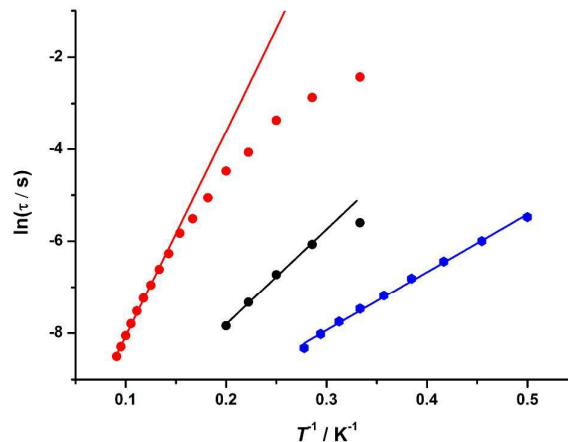


**Fig. 6** The relaxation time is plotted as  $\ln(\tau)$  vs  $T^{-1}$  for **2** (red: low temperature domain; black: high temperature domain) and **3** (blue) under 2000 Oe dc field. The solid lines are fitted using the Arrhenius law.

**1–3** (Fig. 5 and S17). As expected, the QTM was suppressed obviously for **2** and **3** and the full peaks of temperature dependence of ac susceptibility are observed and the frequency-dependent data in the temperature range of 2–11 K for **2** and 2–3.8 K for **3** display the intensity of the  $\chi''$  increases with decreasing the temperature and frequency. Moreover, it is worth noting that the two frequency dependent  $\chi''$  peaks are observed for **2**, which is indicative of double relaxations processes. Multiple relaxation processes have been observed in some reported f-based SMMs mostly due to the existence of different anisotropic centers or isomers and conformers in the crystal. In respective to the structures of **2**, there are two crystallographically independent  $\text{Dy}^{3+}$  centers, which should be responsible for the observation of two relaxations processes (Fig. S18). The presence of two relaxation processes is further examined using a graphical representation,  $\chi''$  versus  $\chi'$  (Cole-Cole plot). The Cole–Cole plots of **2** in the temperature range of 2–12 K exhibits a unique double-ridge shape and the data can be fitted very well via using the sum of two modified Debye functions.<sup>21</sup> The two distinct peaks of the out-of-phase ac signals ( $\chi''$ ) at higher frequencies is evident, which reveals the occurrence of a double relaxation process deriving from two crystallographically independent  $\text{Dy}^{3+}$  centers in **2**.<sup>22</sup> The relaxation time is extracted from the frequency-dependent data based on the Arrhenius law [ $\tau = \tau_0 \exp(U_{\text{eff}}/K_{\text{B}}T)$ ,  $\tau = 1/2\pi f_{\text{max}}$ ] and the Arrhenius plot obtained from these data is given in Fig. 6. The anisotropic energy gaps are calculated to be 20.6 K ( $6.52 \times 10^{-6}$  s) and 44.5 K ( $3.68 \times 10^{-5}$  s) for the low temperature and high temperature domains, respectively for **2**. Meanwhile, the data plotted as Cole-Cole plots of **3** in the temperature range of 2–4 K shows a relatively symmetrical shape and can be fitted to the generalized Debye model (Fig. S19).<sup>22a</sup> The relaxation follows a

thermally activated Orbach mechanism with an energy gap of 12.6 K and a preexponential factor  $\tau_0$  of  $8.14 \times 10^{-6}$  s. It is noted that the  $\tau_0$  values are relatively larger than the expected values for SMM,<sup>24</sup> which is probably enhanced by the presence of quantum tunnelling magnetization.

## Conclusions

In summary, we have solvent-dependently synthesized three Dy-based complexes through the undergoing of solvent exchange, in respect to the coordination of the waters to the Dy<sup>3+</sup> centers in the precursor. Structural analysis indicates the importance of the solvent in different geometry and coordination mode for the as-synthesized products. The structural diversity enables the understanding the crucial role of the solvents in the assembly, crystallization and stability of the supramolecular architectures. The magnetic results of 1–3 highlight the possibility to tune the dynamic behaviours through the adjustment on the structural environment. Especially, ligands in chelating mode would be helpful to strengthen the anisotropic energy barrier in the Dy-bis- $\beta$ -diketonate system.

## Acknowledgements

The authors acknowledge financial support from the NSFC (21572048, 21102039, 21272061 and 51302068), the Open Project of the Key Laboratory of Functional Inorganic Material Chemistry, Heilongjiang University and the Open Project of the State Key Lab of Inorganic Synthesis and Preparative Chemistry, Jilin University.

## Notes and references

- (a) A. Sørensen, A. M. Castilla, T. K. Ronson, M. Pittelkow and J. R. Nitschke, *Angew. Chem. Int. Ed.*, 2013, **52**, 11273–11277; (b) J.-C. G. Bünzli, *Interface Focus*, 2013, **3**, 20130032; (c) W. Xuan, M. Zhang, Y. Liu, Z. Chen and Y. Cui, *J. Am. Chem. Soc.*, 2012, **134**, 6904–6907; (d) M. J. Hannon, *Chem. Soc. Rev.*, 2007, **36**, 280–295; (e) M. Albrecht, *Chem. Rev.*, 2001, **101**, 3457–3497; (f) C. Piguet, G. Bernardinelli and G. Hopfgartner, *Chem. Rev.*, 1997, **97**, 2005–2062.
- (a) Y. Shu, X. Tang and W. Liu, *Inorg. Chem. Front.*, 2014, **1**, 226–230; (b) F. Stomeo, C. Lincheneau, J. P. Leonard, J. E. O'Brien, R. D. Peacock, C. P. McCoy and T. Gunnlaugsson, *J. Am. Chem. Soc.*, 2011, **131**, 9636–9637; (c) B. E. Aroussi, S. Zebret, C. Besnard, P. Perrottet and J. Hamacek, *J. Am. Chem. Soc.*, 2011, **133**, 10764–10767; (d) K. Zeckert, J. Hamacek, J. Senegas, N. Dalla-Favera, S. Floquet, G. Bernardinelli and C. Piguet, *Angew. Chem. Int. Ed.*, 2005, **44**, 7954–7958; (e) J. Yuan, S. Sueda, R. Somazawa, K. Masumoto and K. Matsumoto, *Chem. Lett.*, 2003, **32**, 492–493; (f) A. P. Bassett, S. W. Magennis, P. B. Glover, D. J. Lewis, N. Spencer, S. Parsons, R. M. Williams, L. D. Cola and Z. Pikramenou, *J. Am. Chem. Soc.*, 2004, **126**, 9413–9424.
- (a) P. E. Ryan, L. Guenee and C. Piguet, *Dalton Trans.*, 2013, **42**, 11047–11055; (b) J.-C. G. Bünzli, *Chem. Rev.*, 2010, **110**, 2729–2755; (c) M. Albrecht, O. Osetska, J.-C. G. Bünzli, F. Gumy and R. Frohlich, *Chem. Eur. J.*, 2009, **15**, 8791–8799; (d) A.-S. Chauvin, S. Comby, B. Song, C. D. B. Vandevyver F. Thomas and J.-C. G. Bünzli, *Chem. Eur. J.*, 2007, **13**, 9515–9526; (e) M. Elhabiri, R. Scopelliti, J.-C. G. Bünzli and C. Piguet, *J. Am. Chem. Soc.*, 1999, **121**, 10747–10762; (f) C. Piguet and J.-C. G. Bünzli, in *Handbook on the Physics and Chemistry of Rare Earths*, eds. K. A. Gschneidner Jr, J.-C. G. Bünzli and V. K. Pecharsky, Elsevier Science, Amsterdam, 2010, vol. 40, pp. 301–553.
- (a) T. Zhu, P. Chen, H. Li, W. Sun, T. Gao and P. Yan, *Phys. Chem. Chem. Phys.*, 2015, **17**, 16136–16144; (b) P. Chen, H. Li, W. Sun, J. Tang, L. Zhang and P. Yan, *CrystEngComm*, 2015, **17**, 7227–7232; (c) H. Li, P. Yan, P. Chen, Y. Wang, H. Xu and G. Li, *Dalton Trans.*, 2012, **41**, 900–907; (d) H. Li, G. Li, P. Chen, W. Sun and P. Yan, *Spectrochim. Acta, Part A*, 2012, **97**, 197–201.
- (a) Y. Hui, Y. Meng, Z. Li, Q. Chen, H. Sun, Y. Zhang and S. Gao, *CrystEngComm*, 2015, **17**, 5620–5624; (b) C. Wang, S. Lin, J. Wu, S. Yuan and J. Tang, *Dalton Trans.*, 2015, **44**, 4648–4654; (c) W. Sun, B. Han, P. Lin, H. Li, P. Chen, Y. Tian, M. Murugesu and P. Yan, *Dalton Trans.*, 2013, **42**, 13397–13403; (d) G. Chen, Y. Guo, J. Tian, J. Tang, W. Gu, X. Liu, S. Yan, P. Cheng and D. Liao, *Chem. Eur. J.*, 2012, **18**, 2484–2487; (e) Y. Bi, Y. Guo, L. Zhao, Y. Guo, S. Lin, S. Jiang, J. Tang, B. Wang and S. Gao, *Chem. Eur. J.*, 2011, **17**, 12476–12481.
- (a) P. Zhang, L. Zhang, C. Wang, S. Xue, S. Liu and J. Tang, *J. Am. Chem. Soc.*, 2014, **136**, 4484–4487; (b) L. Jia, Q. Chen, Y. S. Meng, H. Sun and S. Gao, *Chem. Commun.*, 2014, **50**, 6052–6055; (c) D. Yin, Q. Chen, Y. Meng, H. Sun, Y. Zhang and S. Gao, *Chem. Sci.*, 2015, **6**, 3095–3101; (d) Q. Chen, Y. Meng, Y. Zhang, S. Jiang, H. Sun and S. Gao, *Chem. Commun.*, 2014, **50**, 10434–10437; (e) Y. Guo, G. Xu, W. Wernsdorfer, L. Ungur, Y. Guo, J. Tang, H. Zhang, L. F. Chibotaru and A. K. Powell, *J. Am. Chem. Soc.*, 2011, **133**, 11948–11951; (f) W. Sun, B. Yan, Y. Zhang, B. Wang, Z. Wang, J. Jia and S. Gao, *Inorg. Chem. Front.*, 2014, **1**, 503–509; (g) F. Habib, J. Long, P. Lin, I. Korobkov, L. Ungur, W. Wernsdorfer, L. F. Chibotaru and M. Murugesu, *Chem. Sci.*, 2012, **3**, 2158–2164.
- Making Crystals by Design: Methods, Techniques and Applications*, ed. D. Braga and F. Grepioni, Wiley-VCH Verlag GmbH & Co. KGaA, Weinheim, 2007.
- Crystal Design: Structure and Function*, ed. G. R. Desiraju, Wiley, Chichester, 2003.
- (a) J. Martínez-Lillo, D. Armentano, T. F. Mastropietro, M. Julve, J. Faus and G. De Munno, *Cryst. Growth Des.*, 2011, **11**, 1733–1741; (b) P. Kanoo, R. Matsuda, R. Kitaura, S. Kitagawa and T. K. Maji, *Inorg. Chem.*, 2012, **51**, 9141–9143; (c) Y. Tan, A. L. Sudlow, K. C. Molloy, Y. Morishima, K. Fujisawa, W. J. Jackson, W. Henderson, S. N. B. A. Halim, S. W. Ng and E. R. T. Tiekink, *Cryst. Growth Des.*, 2013, **13**, 3046–3056.
- (a) L. Cui, X. Miao, L. Xu, Y. Hu and W. Deng, *Phys. Chem. Chem. Phys.*, 2015, **17**, 3627–3636; (b) D. Frahm, F. Hoffmann and M. Froba, *Cryst. Growth Des.*, 2015, **15**, 1719–1725; (c) J. Duan, M. Higuchi, C. Zou, W. Jin and S. Kitagawa, *CrystEngComm*, 2015, **17**, 5609–5613.
- (a) K. P. Rao, M. Higuchi, J. Duan and S. Kitagawa, *Cryst. Growth Des.*, 2015, **13**, 981–985; (b) P. Gao, Y. Bing and M. Hu, *Inorg. Chem. Commun.*, 2015, **59**, 28–31; (c) L. Zhang, C. Zhang, B. Zhang, C. Du and H. Hou, *CrystEngComm*, 2015, **17**, 2837–2846.
- (a) Y. Ou, Y. Ding, Q. Wei, X. Hong, Z. Zheng, Y. Long, Y. Cai and X. Yao, *RSC Adv.*, 2015, **5**, 27743–27751; (b) M. Hu, Z. Wu, J. Yao, X. Gu and H. Su, *Inorg. Chem. Commun.*, 2013, **36**, 31–34.
- (a) P. Chen, M. Zhang, W. Sun, H. Li, L. Zhao and P. Yan, *CrystEngComm*, 2015, **17**, 5066–5073; (b) M. Zhang, H. Li, P. Chen, W. Sun, L. Zhang and P. Yan, *J. Mol. Struct.*, 2015, **1081**, 233–236; (c) W. Pei, J. Wu, X. Ren, Z. Tian and J. Xie, *Dalton Trans.*, 2012, **41**, 2667–2676.
- (a) D. Chen, X. Ma, X. Zhang, N. Xu and P. Cheng, *Inorg. Chem.*, 2015, **54**, 2976–2982; (b) F. Dai, U. Sambasivam, A. J. Hammerstrom and Z. Wang, *J. Am. Chem. Soc.*, 2014, **136**, 7480–7491; (c) D. Chen, X. Zhang, W. Shi and P. Cheng, *Cryst. Growth Des.*, 2014, **14**, 6261–6268; (d) C. Wan, A. Li, A. A. Al-

- Thabaiti, E. H. El-Mosslamy and T. C. W. Mak, *CrystEngComm*, 2014, **16**, 8960–8968.
- 15 J. Leng, H. Li, P. Chen, W. Sun, T. Gao and P. Yan, *Dalton Trans.*, 2014, **43**, 12228–12235.
- 16 G. M. Sheldrick, *Acta Cryst. C*, 2015, **71**, 3–8.
- 17 H. L. C. Feltham and S. Brooker, *Coord. Chem. Rev.*, 2014, **276**, 1–33.
- 18 (a) R. Zhu, J. Lübben, B. Dittrich and G. H. Clever, *Angew. Chem. Int. Ed.*, 2015, **54**, 2796–2800; (b) W. Colson and W. R. Dichtel, *Nat. Chem.*, 2013, **5**, 453–465; (c) K. Chadwick, J. Chen, A. S. Myerson and B. L. Trout, *Cryst. Growth Des.*, 2012, **12**, 1159–1166; (d) Y. Chang, Z. Lu, L. An and J. Zhang, *J. Phys. Chem. C*, 2012, **116**, 1195–1199.
- 19 (a) M. D. Ward and P. R. Raithby, *Chem. Soc. Rev.*, 2013, **42**, 1619–1636; (b) M. D. Pluth, R. G. Bergman and K. N. Raymond, *Acc. Chem. Soc.*, 2009, **42**, 1650–1659.
- 20 (a) A. Putta, J. D. Mottishaw, Z. Wang and H. Sun, *Cryst. Growth Des.*, 2014, **14**, 350–356; (b) M. Podsiadlo, A. Olenjiczak and A. Katrusiak, *CrystEngComm*, 2014, **16**, 8279–8285; (c) A. J. Cruz-Cabeza and J. Bernstein, *Chem. Rev.*, 2014, **114**, 2170–2191; (d) A. Nangia, *Acc. Chem. Res.*, 2008, **41**, 595–604.
- 21 (a) D. Gatteschi, R. Sessoli and J. Villain, *Molecular Nanomagnets*, Oxford University Press: New York, 2006; (b) S. M. J. Aubin, Z. Sun, L. Pardi, J. Krzystek, K. Folting, L. C. Brunel, A. L. Rheingold, G. Christou and D. N. Hendrickson, *Inorg. Chem.*, 1999, **38**, 5329–5340.
- 22 Y. Guo, G. Xu, P. Gamez, L. Zhao, S. Lin, R. Deng, J. Tang and H. Zhang, *J. Am. Chem. Soc.*, 2010, **132**, 8538–8539.
- 23 (a) Y. Gao, G. Xu, L. Zhao, J. Tang and Z. Liu, *Inorg. Chem.*, 2009, **48**, 11495–11497; (b) F. Tuna, C. A. Smith, M. Bodensteiner, L. Ungur, L. F. Chibotaru, E. J. L. McInnes, R. E. P. Winpenny, D. Collison and R. A. Layfield, *Angew. Chem. Int. Ed.*, 2012, **51**, 6976–6980; (c) F. Pointillart, S. Klementieva, V. Kuropatov, Y. L. Gal, S. Golhen, O. Cadot, V. Cherkasov and L. Ouahab, *Chem. Commun.*, 2012, **48**, 714–716.

**Solvent triggered structural diversity of triple-stranded helicates:****single molecular magnets†**

Hongfeng Li, Peng Chen,\* Wenbin Sun, Lei Zhang and Pengfei Yan\*



Solvents have been found to be the key for the construction of diversified triple-stranded helicates. Distinct solvent molecules are found to coordinate to the Dy<sup>3+</sup> centers in replacement with the original hydrate molecules.